Supporting Information

Rational Design of a Gel-polymer-inorganic Separator with Uniform Lithium-ion Deposition for Highly Stable Lithium-Sulfur Batteries

Pengfei Wang [a], Jiejun Bao [a], Kezhong Lv [a], Na Zhang [a], Zhi Chang [b], Ping He [a], Haoshen Zhou [a,b]**

[a] Center of Energy Storage Materials & Technology, College of Engineering and Applied Sciences, Jiangsu Key Laboratory of Artificial Functional Materials, National Laboratory of Solid State Microstructures, and Collaborative Innovation Center of Advanced Microstructures, Nanjing University, Nanjing 210093, PR China

[b] Energy Technology Research Institute, National Institute of Advanced Industrial Science and Technology (AIST), 1-1-1, Umezono, Tsukuba 305-8568

* Corresponding author: Ping He

E-mail: pinghe@nju.edu.cn

* Corresponding authors: Haoshen Zhou

E-mail: hszhou@nju.edu.cn

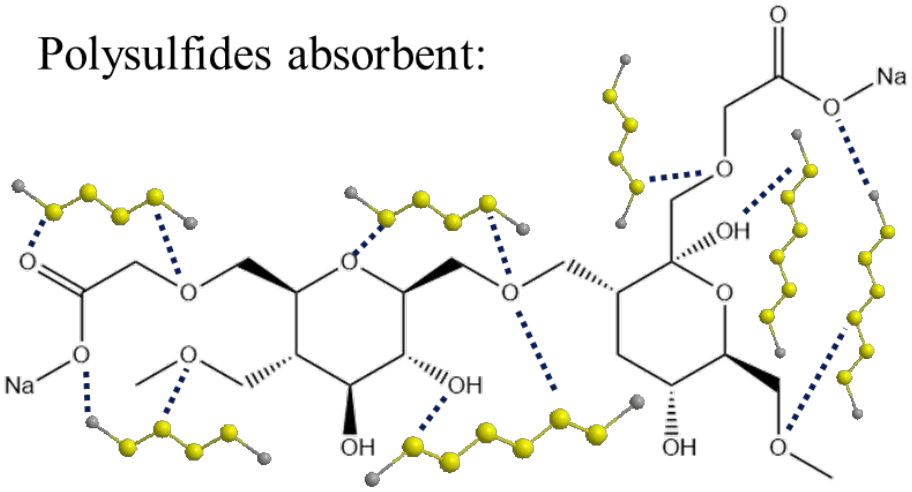

Fig. S1. Schematic illustration of interaction mechanism between polysulfdes and CMC.

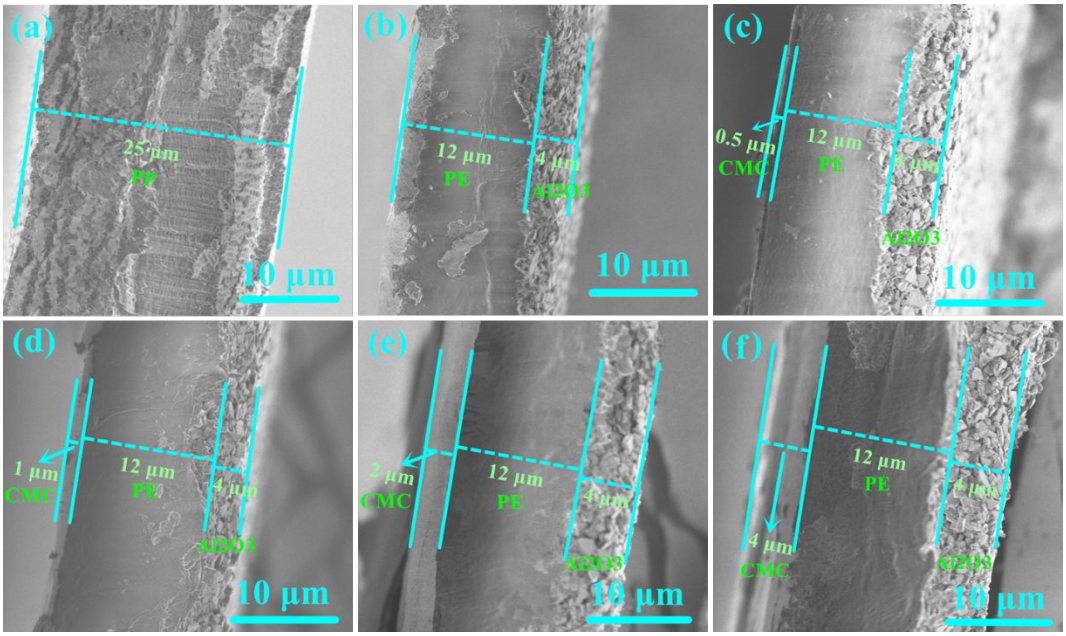

Fig. S2. The cross-section of PP separator (a), Al_2O_3-PE separator (b) and Al_2O_3-PE-CMC separators with different thickness of CMC coating layer (c-f).

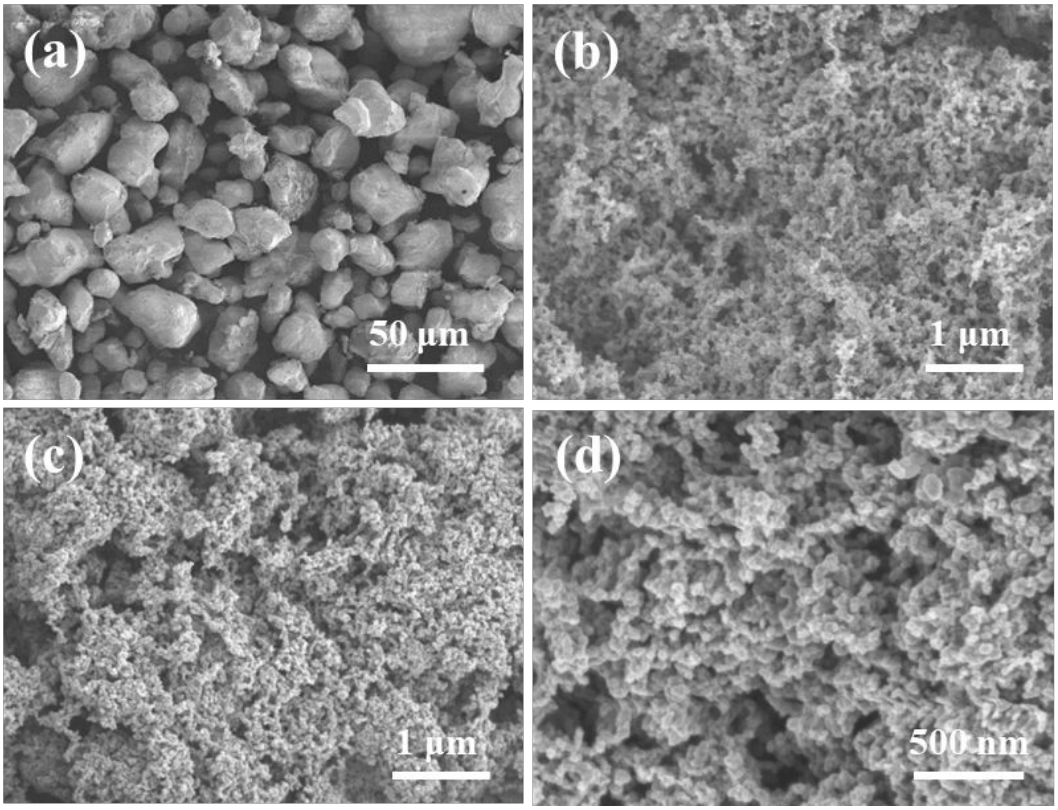

Fig. S3. SEM images of (a) Pure S, (b) Ketjenblack, (c, d) S@Ketjenblack.

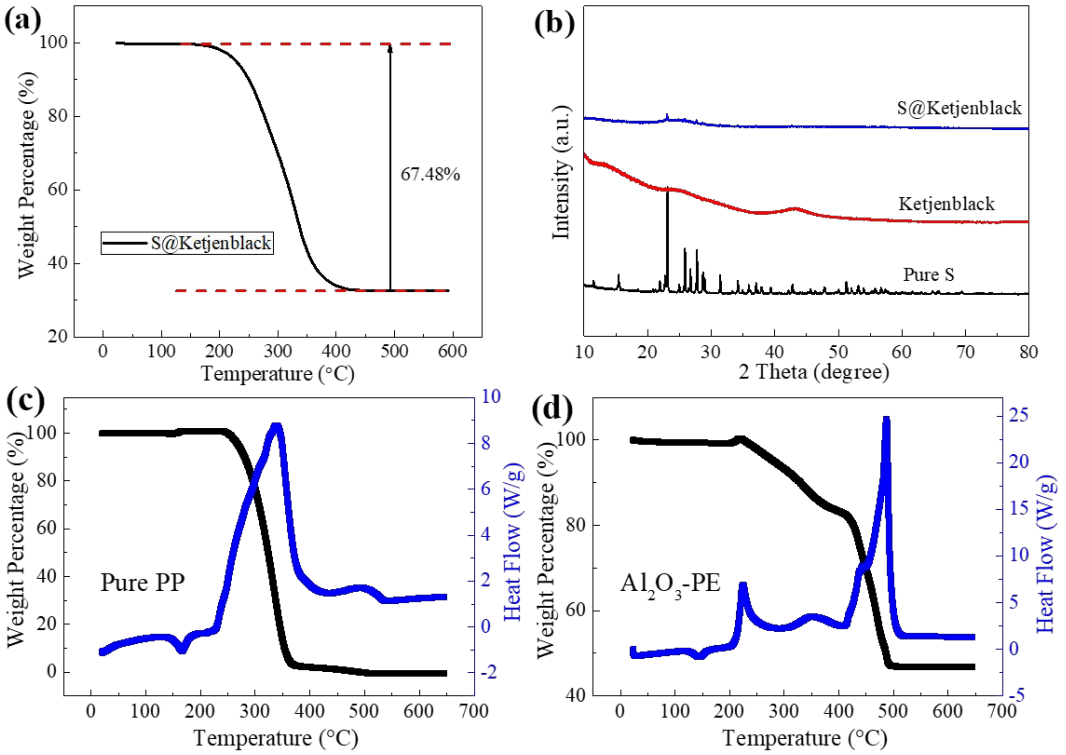

Fig. S4. The TG curve of S@Ketjenblack (a), XRD patterns of S, Ketjenblack and S@Ketjenblack (b), TG-DSC curves of PP (c) and Al_2O_3-PE (d) separator in air atmosphere.

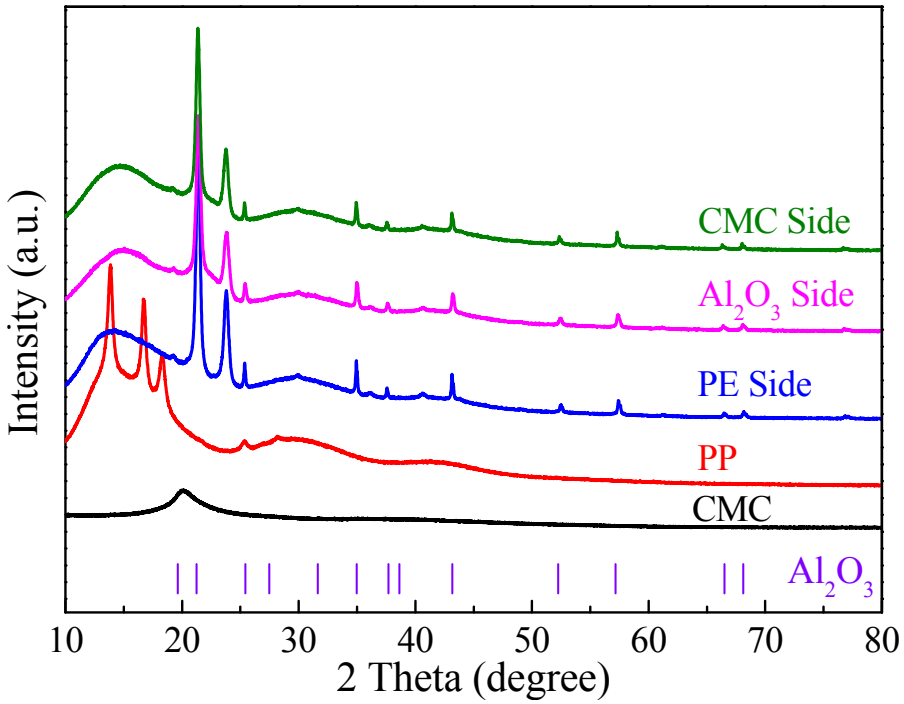

Fig. S5. XRD patterns of different side of PP, PE-Al_2O_3 and CMC-PE-Al_2O_3 separators.

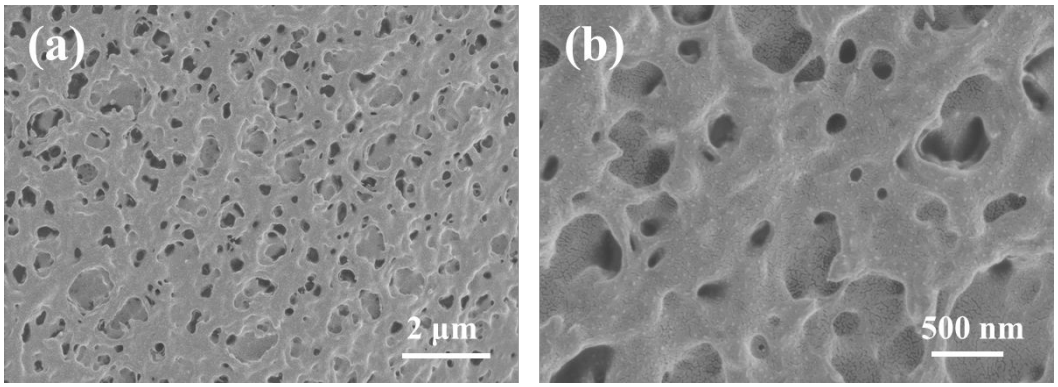

Fig. S6. SEM images of CMC film on the Al_2O_3-PE-CMC separator at different magnifications with the corresponding scale bar of 2 μm (a) and 500 nm (b).

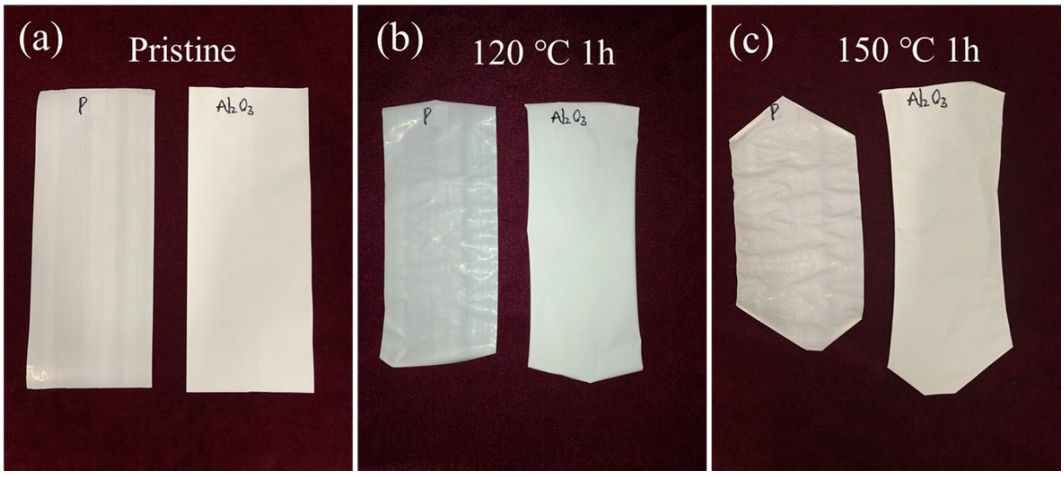

Fig. S7. The thermal stability tests for polymer and Al_2O_3-coated polymer separator (a) pristine, (b) after 120 ℃ for 1h and (c) after 150 ℃ for 1h.

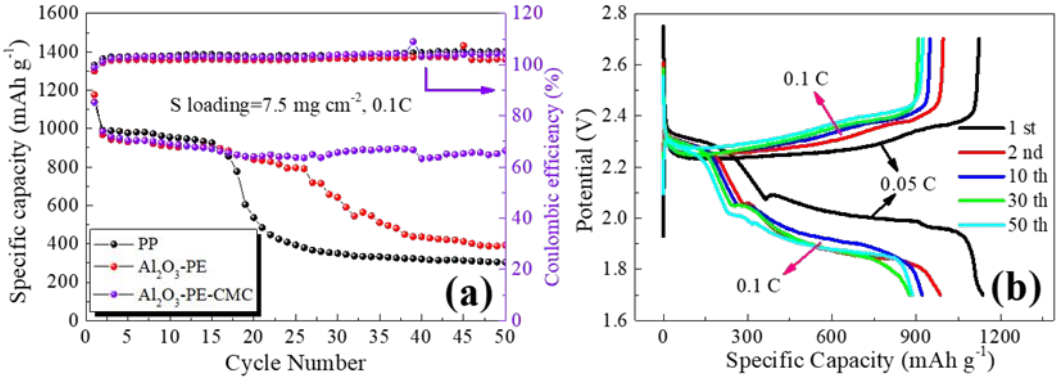

Fig. S8. Cycling performances and coulombic efficiency with high S loading of the PP, Al_2O_3-PE and Al_2O_3-PE-CMC separators in Li-S full cells (a) and Charge/discharge curves of Al_2O_3-PE-CMC separator (b).

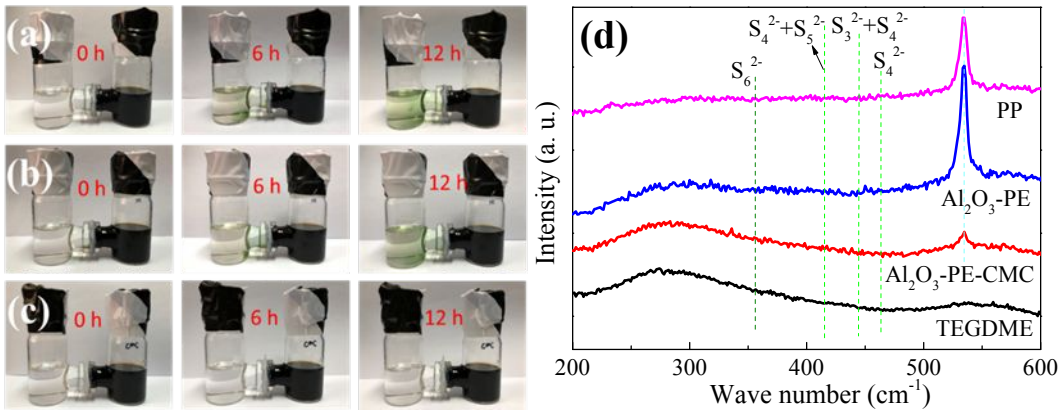

Fig. S9. Polysulfide permeation measurements for the PP (a), Al_2O_3-PE (b) and Al_2O_3-PE-CMC (c) separators during the course of polysulfide diffusion from the right side to the left side of the H-shaped glass bottles, the Raman spectra of the pure TEGDME and the polysulfide solution in the left side after 12 h (d).

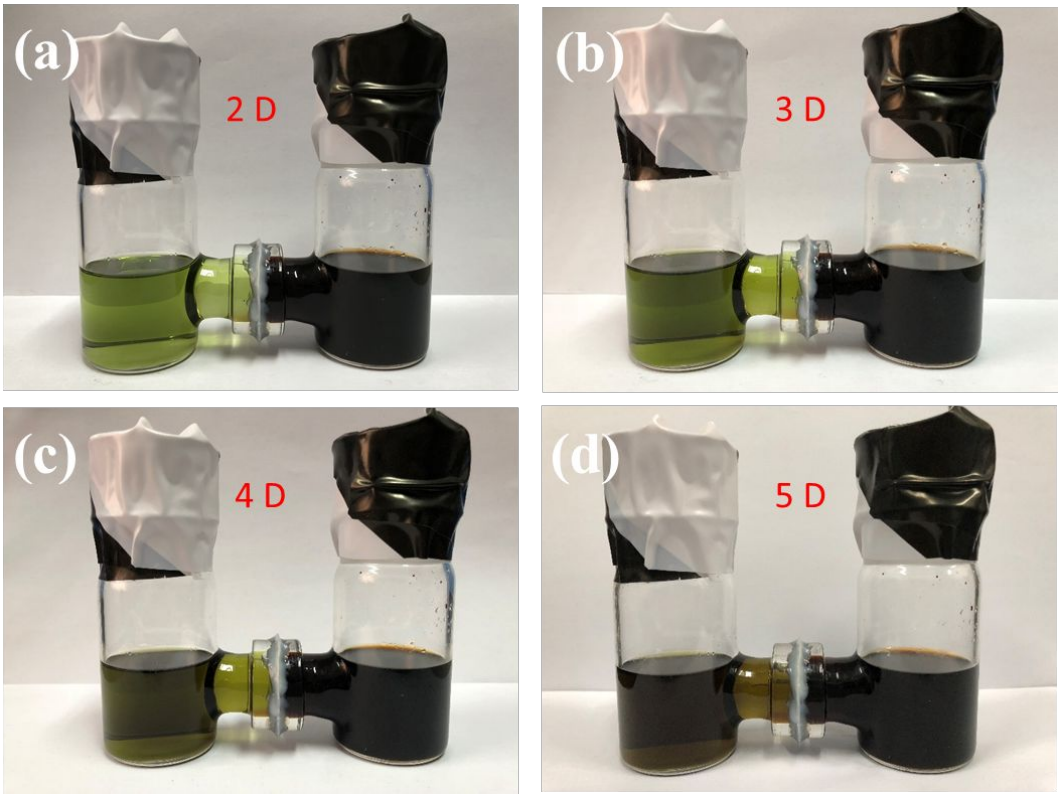

Fig. S10. Polysulfide permeation measurement for the PP separator after (a) 2 days, (b) 3 days, (c) 4 days and (d) 5 days.

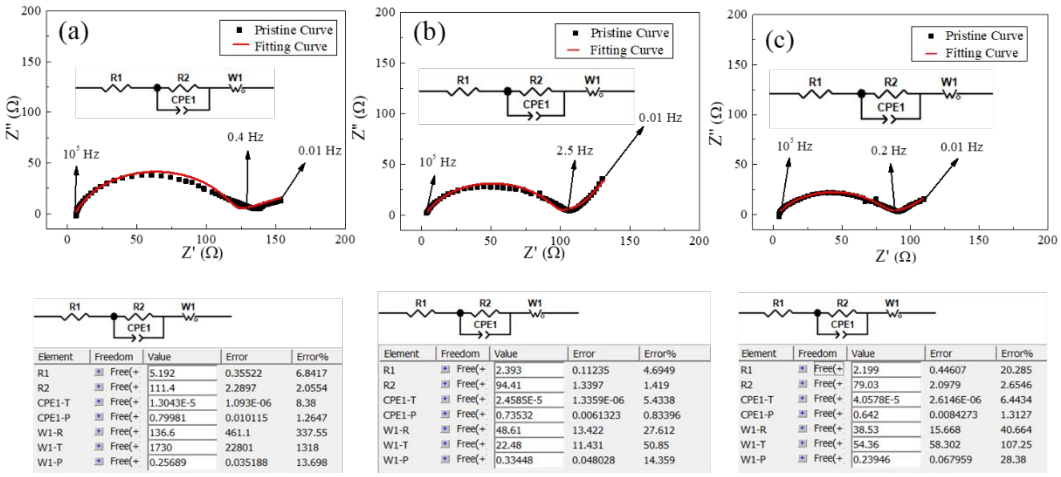

Element	Freedom	Value	Error	Error%
R1	Free(+	5.192	0.35522	6.8417
R2	Free(+	111.4	2.2897	2.0554
CPE1-T	Free(+	1.3043E-5	1.093E-06	8.38
CPE1-P	Free(+	0.79981	0.010115	1.2647
W1-R	Free(+	136.6	461.1	337.55
W1-T	Free(+	1730	22801	1318
W1-P	Free(+	0.25689	0.035188	13.698

Element	Freedom	Value	Error	Error%
R1	Free(+	2.393	0.11235	4.6949
R2	Free(+	94.41	1.3397	1.419
CPE1-T	Free(+	2.4585E-5	1.3359E-06	5.4338
CPE1-P	Free(+	0.73532	0.0061323	0.83396
W1-R	Free(+	48.61	13.422	27.612
W1-T	Free(+	22.48	11.431	50.85
W1-P	Free(+	0.33448	0.048028	14.359

Element	Freedom	Value	Error	Error%
R1	Free(+	2.199	0.44607	20.285
R2	Free(+	79.03	2.0979	2.6546
CPE1-T	Free(+	4.0578E-5	2.6146E-06	6.4434
CPE1-P	Free(+	0.642	0.0084273	1.3127
W1-R	Free(+	38.53	15.668	40.664
W1-T	Free(+	54.36	58.302	107.25
W1-P	Free(+	0.23946	0.067959	28.38

Fig. S11. Specific fitting results from the EIS of PP (a), Al_2O_3-PE (b) and Al_2O_3-PE-CMC (c) separators in Li-S full cells.

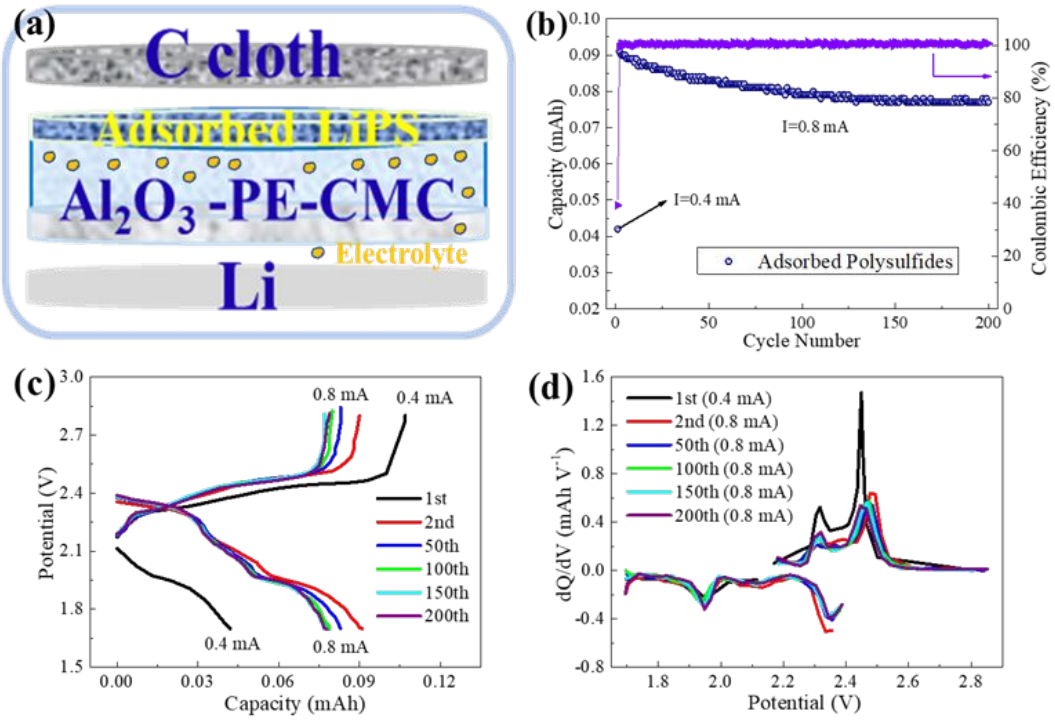

Fig. S12. The structure schematic of the battery using Al_2O_3-PE-CMC separator anchored with polysulfides and C cloth as cathode (a), the corresponding cycling performance (b), charge/discharge curves (c) and differential capacity curves (d).